

# Combination of thermionic emission and tunneling mechanisms to analyze the leakage current in 4H-SiC Schottky barrier diodes

A. Latreche

*Département des sciences de la matière, Université de Bordj Bou Arreridj, Algeria*

\* E-mail: hlat26@yahoo.fr

**Abstract.** A new method to analyze reverse characteristics of 4H-SiC Schottky barrier diode has been presented in this paper. The model incorporates both the current induced by the tunneling of carriers through the Schottky barrier and that induced by the thermionic emission of carriers across the metal–semiconductor interface. The treatment includes the effect of image force lowering both the thermionic emission and electron tunneling processes. This analysis allowed us to separate and identify the thermionic emission and tunneling components of the total current. The experimental reverse transition voltage between thermionic emission and tunneling process can be determined from the intersection of the two components by using two models; bias dependence and no bias dependence of barrier height. For high temperatures, the experimental reverse transition voltage increases with increasing the temperature and decreases with increasing the doping concentration as predicted by Latreche’s model.

**Keywords:** reverse transition voltage, thermionic emission, tunneling current, SiC Schottky diode, image force barrier lowering.

doi: doi: <https://doi.org/10.15407/spqeo22.01.19>

PACS 85.30.De, 85.30.Kk, 85.30.Mn

Manuscript received 20.12.18; revised version received 01.02.19; accepted for publication 20.02.19; published online 30.03.19.

## 1. Introduction

The wide bandgap semiconductor silicon carbide (4H-SiC) is attractive in a wide range of application fields, namely: high-power, high-temperature and high-frequency electronic devices because of its excellent material properties. The SiC material properties that make it suitable to replace silicon in high power devices include wider band gap, large breakdown fields, high thermal conductivity and acceptable bulk mobility [1-4]. In the recent years, Schottky barrier diode (SBD) based on 4H-SiC has been studied regarding its fast switching capability and transport mechanisms. Under the reverse-bias condition, the dominant mechanisms by which carrier transport occurs in Schottky barriers are thermionic emission and carrier tunneling through the potential barrier [5]. Both models were used separately to analyze the experimental reverse leakage current of SiC and other wide-gap SBDs. Combined and not combined with barrier lowering model, some authors [6-11] described the reverse leakage current using the general model [12] of the tunneling current. At the same time, the others [13-18] used the thermionic field emission (TFE) developed by Padovani–Stratton [19] also with

and without the effect of the image force barrier lowering. However, some researchers [20-22] used thermionic emission model in combination with the barrier lowering one to describe the experimental reverse characteristics data. In fact, the total current through SBD is the sum of both these mechanisms: thermionic emission and tunneling process [9, 23]. In his more recent theoretical work, Latreche [24] showed the importance of taking into account the both mechanisms for analysis of reverse leakage current of 4H-SiC SBDs. In this study, the author proposes a combined model to analyze the leakage current of 4H-SiC Schottky diodes, which takes into account in a common framework these two main sources of leakage current present in Schottky diodes, namely, the current caused by thermionic emission and that caused by the tunneling of carriers through the Schottky barrier. Both these models are combined with the barrier lowering model. This new method will allow us to separate the two components of the total current; hence, we can experimentally determine the reverse transition voltages between these two contributing mechanisms and, then, we compare them with those calculated using the Latreche model [24].

## 2. Theory and modeling

Thermionic emission over the potential barrier and carrier tunneling through potential barrier are two dominant mechanisms by which the carrier transport occurs in Schottky barriers [5]. The total current density flowing through the Schottky potential barrier, which consists of both thermionic emission and tunneling, can be conveniently expressed according to the Tsu–Esaki formalism as [7, 9, 12, 23]

$$J_{Tun} = \frac{A^*T}{k_B} \int_0^{\infty} T(E_x) \ln \left( \frac{1 + \exp(-q\zeta - E_x)/k_B T}{1 + \exp(-q\zeta - qV_R - E_x)/k_B T} \right) dE_x \quad (1)$$

where  $A^*$  is the effective Richardson constant,  $T$  – temperature,  $k_B$  – Boltzmann constant,  $\zeta$  denotes the difference between the equilibrium Fermi level and conduction bands, and  $T(E_x)$  is the tunneling probability calculated using the WKB approximation:

$$T_{WKB}(E_x) = \exp \left[ -2 \int_{x_1}^{x_2} \left( \frac{2m^*}{\hbar^2} (U(x) - E_x) \right)^{1/2} dx \right]. \quad (2)$$

Here,  $x_1$  and  $x_2$  are the two turning points. The WKB approximation could reasonably predict tunneling current through the Schottky barrier with and without the effect of lowering the image barrier [25]. When the effect of lowering the force barrier is taken into account, the potential energy of the Schottky barrier  $U(x)$  measured from the bottom edge of the conduction band in the bulk of the semiconductor is [9, 26]:

$$U(x) = \frac{q^2 N_D}{2\epsilon_S} (D - x)^2 - \frac{q^2}{16\pi\epsilon_S x}, \quad (3)$$

where  $\epsilon_S$  is the semiconductor permittivity,  $N_D$  – doping density,  $D$  – depletion width dependent on reverse bias voltage  $V_R$ .

In the current expression (1), both these mechanisms of the conduction carriers flow in SBD are included: thermionic emission occurs for energy higher than the maximum of the potential Schottky barrier ( $E_x > U_{max}$ ), and the tunneling process occurs for the lower energy range ( $E_x < U_{max}$ ) [9, 23]:

$$J_{Tot} = J_{Tun} + J_{Therm}, \quad (4)$$

where the reverse tunneling current density is given by [7, 9, 12, 23]

$$J_{Tun} = \frac{A^*T}{k_B} \int_0^{U_{max}} T(E_x) \ln \left( \frac{1 + \exp(-q\zeta - E_x)/k_B T}{1 + \exp(-q\zeta - qV_R - E_x)/k_B T} \right) dE_x \quad (5)$$

and the thermionic emission current density with including the image force decrease is expressed by [9, 23]:

$$J_{Therm} = \frac{A^*T}{k_B} \int_{U_{max}}^{\infty} T(E_x) \ln \left( \frac{1 + \exp(-q\zeta - E_x)/k_B T}{1 + \exp(-q\zeta - qV_R - E_x)/k_B T} \right) dE_x. \quad (6)$$

When the effect of lowering the image force is taken into account, by setting the tunneling probability  $T(E_x) = 1$  for the energies higher than the maximum of the Schottky potential barrier and approximating the Fermi–Dirac statistics with the Maxwell–Boltzmann one, Eq. (6) of the thermionic emission current can be rewritten as [9, 23]

$$J_{Therm} = A^*T^2 e^{-\frac{q}{k_B T}(\phi_b - \Delta\phi_b)} \left( \frac{qV}{e^{k_B T} - 1} \right), \quad (7)$$

where the image force decrease is given by [27]:

$$\Delta\phi_b = \left[ \frac{q^3 N_D (\phi_b - \zeta - V_R)}{8\pi^2 \epsilon_S^3} \right]^{1/4}. \quad (8)$$

In order to predict the reverse transition voltage between thermionic emission and tunneling process as a function of temperature, doping concentration and barrier height for 4H-SiC Schottky barrier diode, the analytical model was proposed by Latreche [24]:

$$V_T \approx \begin{cases} \left[ \frac{[f(\phi_b) + g(\phi_b)T + h(\phi_b)T^2 + p(\phi_b)T^3] 10^{15}}{N_D} \right]^{1/4} \\ \text{for } 50 \text{ K} \leq T \leq T_2 = 300\phi_b \\ \left[ \frac{[137.301 - 1.04T + 2.8210^{-3}T^2] 10^{15}}{N_D} \right]^{1/4} \\ \text{for } T > T_2 = 300\phi_b \end{cases} \quad (9)$$

where the functions  $f(\phi_b)$ ,  $g(\phi_b)$ ,  $h(\phi_b)$  and  $p(\phi_b)$  are given by

$$\begin{cases} f(\phi_b) = -39.027 + 85.179\phi_b \\ g(\phi_b) = 6.13410^{-2} - 1.548\phi_b \\ h(\phi_b) = (11.124 + 23.13\phi_b)10^{-3} \\ p(\phi_b) = (-114.836 + 18.5\phi_b)10^{-6} \end{cases} \quad (10)$$

To extract barrier height ( $\phi_b$ ) from the reverse  $I$ - $V$  characteristic, we propose two models. The first one assumes that the barrier height  $\phi_b$  is bias-dependent due to the presence of an interfacial layer and interface states located at the contact between metal and semiconductor

[28, 29]. In this case, the following equation can be solved numerically by using the Newton method:

$$J_{theor}^j(V_j) = J_{Tun}^j(V_j) + J_{Therm}^j(V_j) = J_{exp}^j(V_j). \quad (11)$$

Here,  $J_{exp}^j(V_j)$  is the reverse current density for each bias voltage measurement,  $J_{Tun}^j(V_j)$  and  $J_{Therm}^j(V_j)$  are the theoretical components of the current given by Eqs (5) and (7), respectively.

The second model assumes that the effective barrier height is independent of applied bias, and it can be determined from the first model by calculating the average value of the barrier height values calculated for each bias voltage measurement.

### 3. Results and discussion

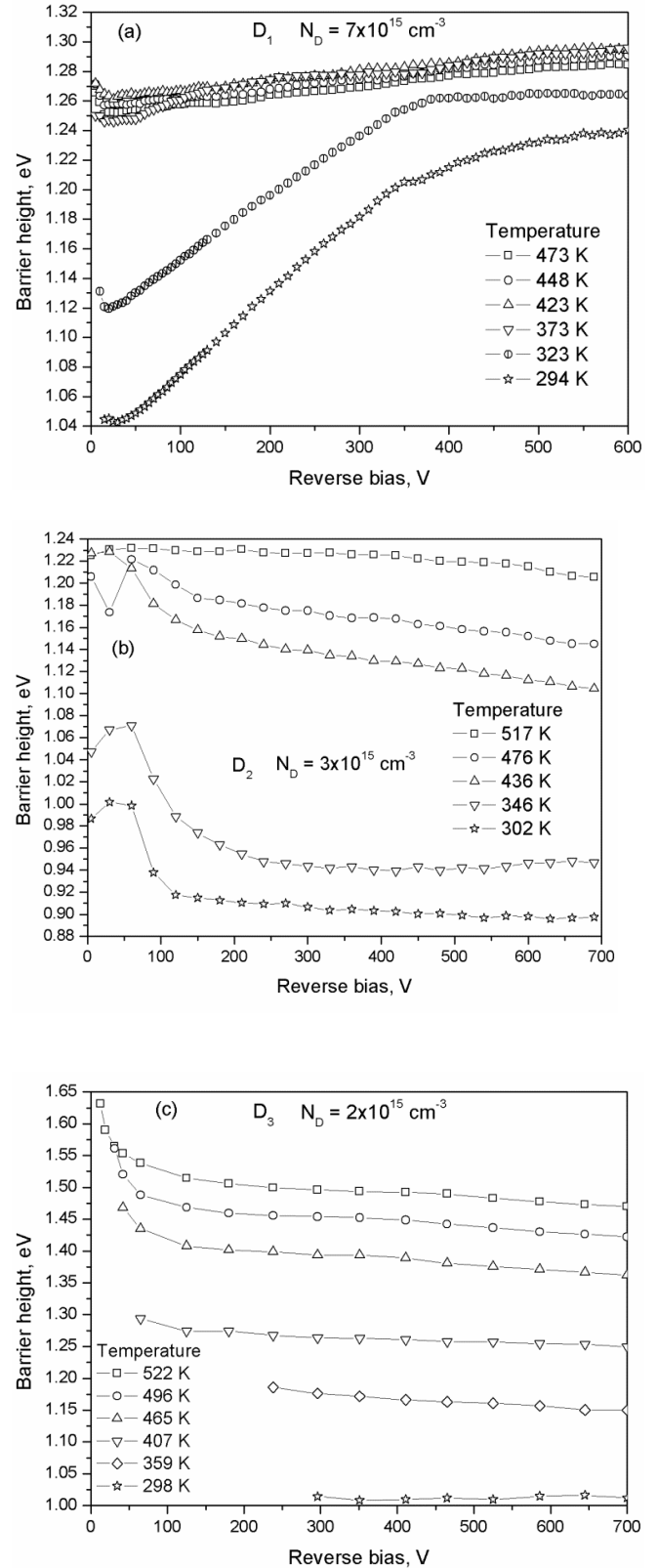
In order to apply our new method, we used the experimental data on silicon carbide (4H-SiC) previously published in the literature by several authors [13, 30, 31]. The wafers had an *n*-type epitaxial layer. The type of diode, doping concentration  $N_D$  and temperatures are summarized in Table. The values of Richardson's constant and effective masses were taken as follows:  $146 \text{ A}\cdot\text{cm}^{-2}\cdot\text{K}^{-1}$  and  $m^* = 0.2m_0$ , respectively [32, 33].

Fig. 1 shows the extracted barrier height as a function of the reverse bias for 4H-SiC Schottky barrier diodes at various temperatures, when both these mechanisms are combined. In the case of diode  $D_1$  (Fig. 1a), where the doping concentration is  $7 \cdot 10^{15} \text{ cm}^{-3}$ , the barrier height increases slightly with increasing the reverse bias within the high temperatures range 373...473 K. However, in the case of these two low temperatures 323 and 294 K, the barrier height increases with increasing the reverse bias in particular for reverse bias less than 380 V, whilst beyond this value the barrier height increases slightly with increasing the reverse bias.

In the case of two diodes  $D_2$  and  $D_3$ , where the doping concentrations are  $3 \cdot 10^{15}$  and  $2 \cdot 10^{15} \text{ cm}^{-3}$ , respectively, the barrier height decreases slightly for all the temperatures for the high reverse bias ( $> 200 \text{ V}$  for  $D_2$  and  $> 100 \text{ V}$  for  $D_3$ ), while for low temperatures the barrier height is strongly decreased at low reverse bias. For three these diodes, the barrier height decreases with decreasing the temperature. We noted that for SiC SBDs the Schottky barrier height strongly depends on the reverse bias voltage, temperature and doping concentration [10]. These dependences are caused by combination of the effects of the interfacial layer and interface states located at the contact interface between metal and semiconductor [10].

Fig. 2 shows experimental and calculated reverse current densities according to tunneling and thermionic models for 4H-SiC Schottky diode  $D_2$  at various temperatures by using the first model that assumes bias dependence of barrier height (model 1). The calculated reverse current densities are obtained using the

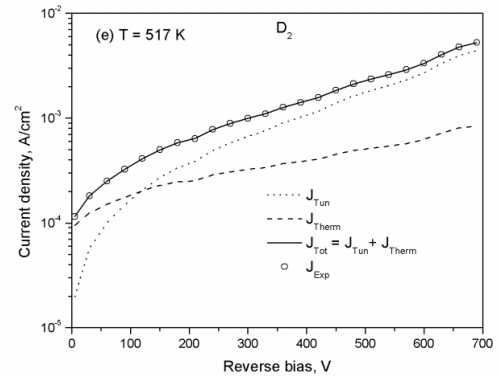
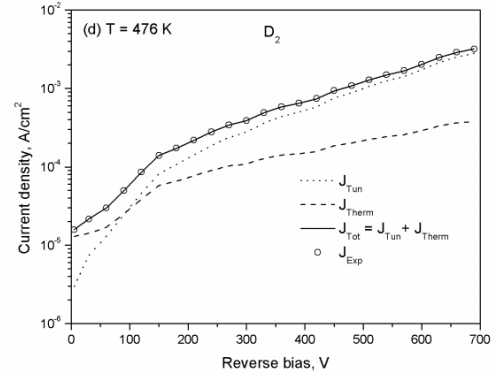
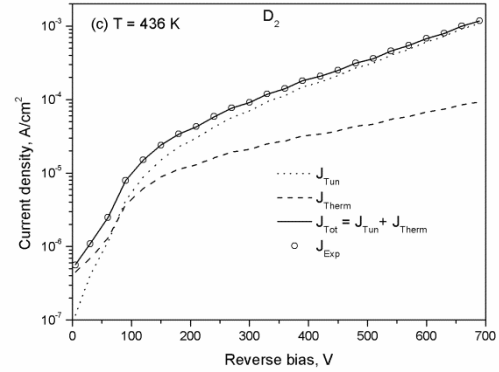
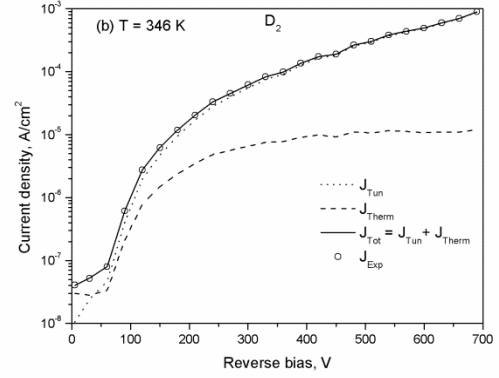
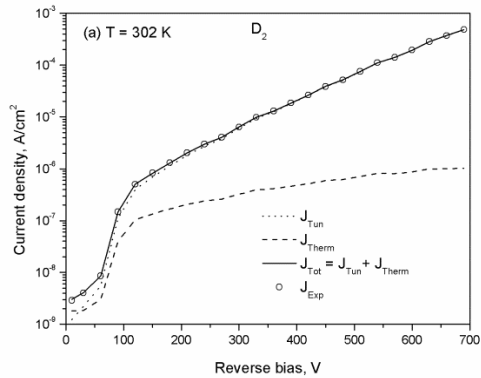
corresponding extracted barrier height which is plotted in Fig. 1b. The intersection between the components of thermionic emission and tunneling currents represents



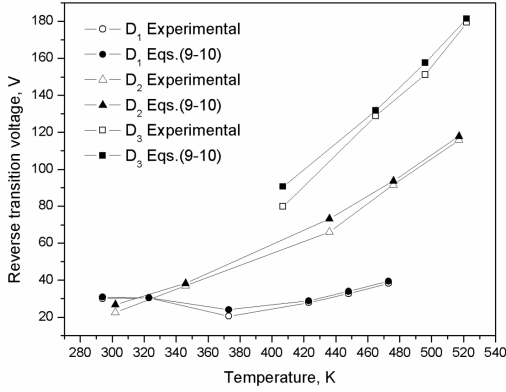
**Fig. 1.** Schottky barrier height as a function of the reverse bias voltage at various temperatures for 4H-SiC SBDs.

the reverse transition voltage ( $V_T$ ) between both corresponding mechanisms. The thermionic emission component is seen to be dominant for low voltages up to about  $V_T$ , whereas the tunneling mechanism becomes dominant for the biases higher than  $V_T$ . Near the reverse transition voltage, neither tunneling nor thermionic emission accurately describes the conduction process, because both these currents have the same order of magnitude, and, therefore, both these mechanisms should be combined together to analyze the reverse  $I$ - $V$  characteristics. In this model, where the barrier height is extracted from each data ( $I_i$ - $V_i$ ), the total current that presents the sum of two these components have the same value as the experimental one. Fig. 3 shows comparison of experimental reverse transition voltage with calculated results obtained by using the Latreche model presented by equations (9) and (10) for all diodes. It can be seen in Fig. 3 that the experimental values of  $V_T$  of this work shows good agreement with the calculated values within the whole temperature range for all the diodes. As predicted by Latreche's model (Eqs (9) and (10)), the experimental reverse transition voltage decreases when the doping concentration is increased, and also the reverse transition voltage increases with increasing the temperature in the high temperature range on the parabolic shape, wherever the value of the barrier height. At low temperatures, the Latreche model predicts a peak that is absent in this study due to the high temperatures used in the experiments. In this context, it may be noted that for low temperatures the barrier height will decrease, hence, the current will be small, difficult to measure, in particular at lower reverse bias where probably the transition between thermionic emission and tunneling process may occur. In the case of diode  $D_1$ , the reverse transition voltage increases from 20.6 V at the temperature 373 K to 30.5 V at the temperature 323 K.

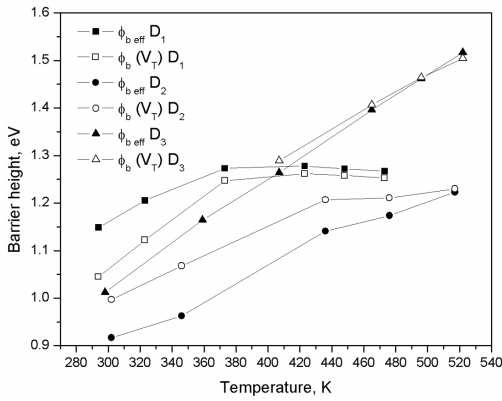
Comparison between the barrier height corresponding to the reverse transition voltage  $\phi_b(V_T)$  extracted using model 1 (barrier height is bias-dependent) and the effective barrier height  $\phi_{b\text{eff}}$  is shown in Fig. 4. It can be seen in this figure that  $\phi_b(V_T)$



**Fig. 2.** Reverse  $J$ - $U$  characteristics based on both thermionic emission and tunneling process for 4H-SiC SBD;  $D_2$  for various temperatures. Experimental data are also shown. The calculated  $J$ - $U$  characteristics are resulting, if using the extracted barrier height plotted in Fig. 1b.

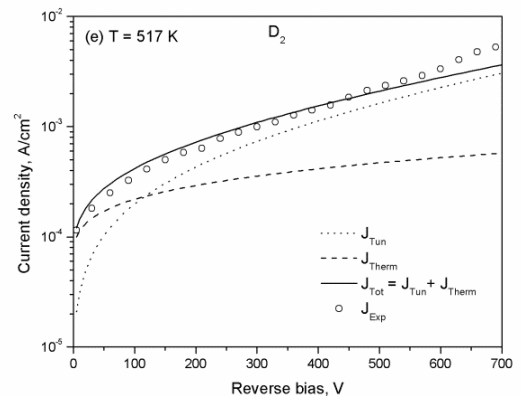
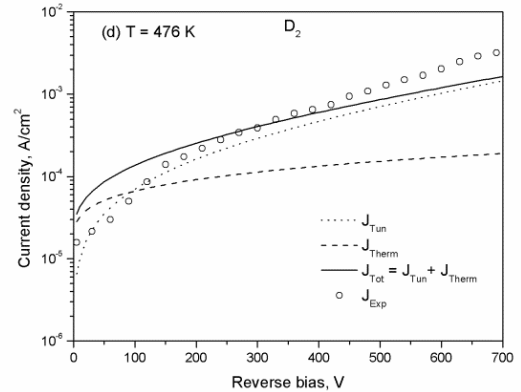
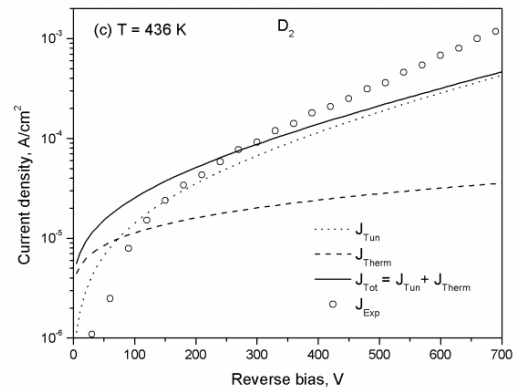
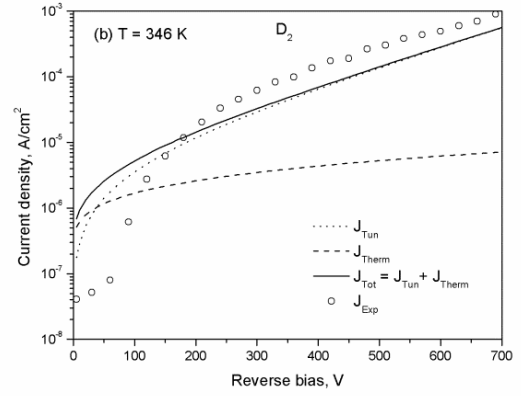
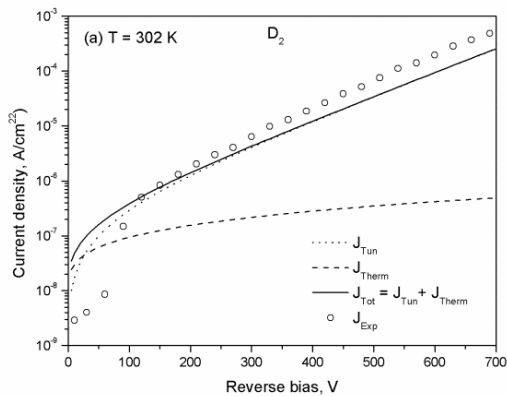


**Fig. 3.** Experimental reverse transition voltage as a function of temperature for 4H-SiC Schottky barrier diodes. Comparison with the calculated reverse transition voltage by using Latreche's model (Eqs. (9) and (10)).



**Fig. 4.** Effective barrier height as a function of temperature for 4H-SiC SBDs. Comparison with the barrier height corresponding to the reverse transition voltage  $\phi_b(V_T)$ .

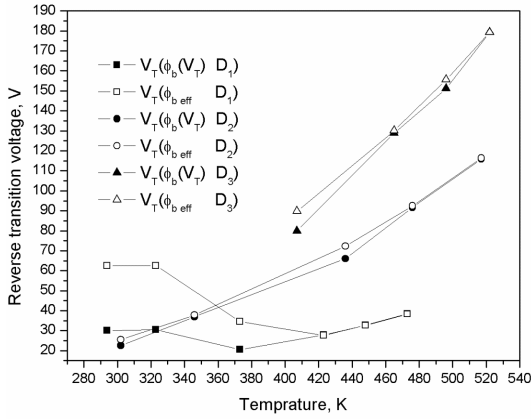
is in good agreement with  $\phi_{b,eff}$  for high temperatures, while this agreement becomes worse at low temperatures due to the strong bias dependence of the barrier height at low reverse bias for low temperatures, as we have shown above. In the case of diode  $D_2$ ,  $\phi_b(V_T)$  is not shown in Fig. 4 for low temperatures, because the  $I$ - $V$  data are not available at lower reverse biases where probably the transition between thermionic emission and tunneling process may occur (see Fig. 2a in Ref. [31]).



**Fig. 5.** Reverse  $J$ - $U$  characteristics based on both the thermionic emission and tunneling process for 4H-SiC SBD;  $D_2$  for various temperatures. Experimental data are also shown. The calculated  $J$ - $U$  characteristics are resulting, if using the extracted effective barrier height  $\phi_{b,eff}$  plotted in Fig. 4 ( $D_2$ ).

**Table.** Some properties of SiC diodes collected from several works.

Type	Symbol	Concentration $N_D$ (cm <sup>-3</sup> )	Temperature $T$ (K)	Reference
Ti/4H-SiC	D <sub>1</sub>	$\sim 7 \cdot 10^{15}$	294–473 K	[13]
Ni <sub>2</sub> Si/4H-SiC	D <sub>2</sub>	$3 \cdot 10^{15}$	302–517 K	[30]
Ni/4H-SiC	D <sub>3</sub>	$2 \cdot 10^{15}$	298–522 K	[31]


**Fig. 6.** Experimental reverse transition voltages as functions of temperature extracted by using bias dependence and no bias dependence of barrier height models for SiC SBDs.

Shown in Fig. 4 are the experimental and calculated reverse current densities according to tunneling and thermionic models for 4H-SiC Schottky diode D<sub>2</sub> at various temperatures using the second model that assumes no bias dependence of barrier height. As can be seen from this figure, the total current is in good agreement with experimental data, especially for higher temperatures. The discrepancies between calculation and experiment become large at low temperatures. This observation was reported in several works in the literature [6, 13, 14, 18] because the barrier height is strongly dependent on the reverse bias (first model), especially at lower temperatures. Thus, we can conclude that the first model which assumes bias dependence is more appropriate than the second one that assumes no bias dependence for analysis of the reverse characteristics of the 4H-SiC Schottky barrier diodes and other wide bandgap SBDs.

The experimental reverse transition voltage between the thermionic and tunneling currents for these two models (bias and no bias dependence) are plotted in Fig. 5. The values of the reverse transition voltage for these two models have practically the same values over all the temperature ranges for the diode D<sub>2</sub>. However, for the diode D<sub>1</sub> the agreement becomes worse at low temperatures.

#### 4. Conclusion

Our study has been based on the reverse current model that incorporates in a unified way both the current due to the thermionic emission of carriers across metal–

semiconductor interface and the tunneling current through the potential barrier. By means of the analytical method of the model, the different contributions to the net current of the 4H-SiC Schottky barrier diode have been identified from the  $I$ - $V$  experimental data previously published in the literature. The reverse transition voltage ( $V_T$ ) between thermionic emission and tunneling currents represents the value of the intersection of the both curves  $I$ - $V$  of the two components. Two models have been used to analyze experimental data such as bias dependence and no bias dependence of barrier height. It has been shown that bias dependence of barrier height model is more appropriate to describe leakage current of Schottky barrier diode, in particular at low temperatures and low reverse bias, because in these ranges the barrier height is strongly dependent on temperature and reverse bias. The experimental reverse transition voltage was found to increase with decreasing the doping concentration and increase with increasing temperatures as predicted by Latreche's model.

#### References

1. Mahajan A. and Skromme B.J. Design and optimization of junction termination extension (JTE) for 4H-SiC high voltage Schottky diodes. *Solid-State Electron.* 2005. **49**. P. 945–955.
2. Matsunami H. Current SiC technology for power electronic devices beyond Si. *Microelectron. Eng.* 2006. **83**. P. 2–4.
3. Kimoto T. Material science and device physics in SiC technology for high-voltage power devices. *Jpn. J. Appl. Phys.* 2015. **54**. P. 040103.
4. Privitera S.M.S., Latrice G., Camarda M., Piluso N., and La Via F. Electrical properties of extended defects in 4H-SiC investigated by photoinduced current measurements. *Appl. Phys. Express.* 2017. **10**. P. 036601.
5. Rhoderick E.H. Metal-semiconductor contacts. *IEE PROC.* 1982. **129**. P. 1–14.
6. Crofton J. and Sriram S. Reverse leakage current calculations for SiC Schottky contacts. *IEEE Trans. Electron. Devices.* 1996. **43**. P. 2305–2307.
7. Eriksson J., Rorsman N. and Zirath H. 4H-silicon carbide Schottky barrier diodes for microwave applications *IEEE Trans. Microwave Theory Technol.* 2003. **51**. P. 796–804.

8. Blasciuc-Dimitriu D., Horsfall A. B., Wright N.G., et al. Quantum modelling of I–V characteristics for 4H–SiC Schottky barrier diodes. *Semicond. Sci. Technol.* 2005. **20**. P. 10–15.
9. Furno M., Bonani F. and Ghione G. Transfer matrix method modelling of inhomogeneous Schottky barrier diodes on silicon carbide. *Solid-State Electron.* 2007. **51**. P. 466–474.
10. Latreche A. Reverse bias-dependence of Schottky barrier height on silicon carbide: influence of the temperature and donor concentration. *Int. J. Phys. Res.* 2014. **2**. P. 40–49.
11. Okino H., Kameshiro N., Konishi K. et al. Analysis of high reverse currents of 4H–SiC Schottky-barrier diodes. *J. Appl. Phys.* 2017. **122**. P. 235704.
12. Tsu R. and Esaki L. Tunneling in a finite superlattice. *Appl. Phys. Lett.* 1973. **22**. P. 562–564.
13. Treu M., Rupp R., Kpels H. and Bartsch W. Temperature dependence of forward and reverse characteristics of Ti, W, Ta and Ni Schottky diodes on 4H–SiC. *Mater. Sci. Forum.* 2001. **353-356**. P. 679–682.
14. Oyama S., Hashizume T. and Hasegawa H. Mechanism of current leakage through metal/*n*-GaN interfaces. *Appl. Surf. Sci.* 2002. **190**. P. 322–325.
15. Hatakeyama T., Kushibe M., Watanabe T., Imai S. and Shinohe T. Optimum design of a SiC Schottky barrier diode considering reverse leakage current due to tunneling process. *Mat. Sci. Forum.* 2003. **433-436**. P. 831–834.
16. Xie K., Hartz S.A., Ayres V.M. et al. Thermionic field emission in GaN nanoFET Schottky barriers. *Mater. Res. Express.* 2015. **2**. P. 015003.
17. Kim H. Reverse-bias leakage current mechanisms in Cu/*n*-type Schottky junction using oxygen plasma treatment. *Trans. Electr. Electron. Mater.* 2016. **17**. P. 113–117.
18. Higashiwaki M. et al. Temperature-dependent capacitance–voltage and current–voltage characteristics of Pt/Ga<sub>2</sub>O<sub>3</sub> (001) Schottky barrier diodes fabricated on *n*-Ga<sub>2</sub>O<sub>3</sub> drift layers grown by halide vapor phase epitaxy. *Appl. Phys. Lett.* 2016. **108**. P. 133503.
19. Padovani F.A. and Stratton R. Field and thermionic-field emission in Schottky barriers. *Solid-State Electron.* 1962. **9**. P. 695–707.
20. Ivanov P.A., Grekhov I.V., Kon'kov O.I. et al. I–V characteristics of high-voltage 4H–SiC diodes with a 1.1-eV Schottky barrier. *Semiconductors.* 2011. **45**. P. 1374–1377.
21. Ivanov P.A., Grekhov I.V., Potapov A.S. et al. Reverse leakage currents in high-voltage 4H–SiC Schottky diodes. *Mater. Sci. Forum.* 2013. **740-742**. P. 877–880.
22. Lee K.Y., Liu Y.H., Wang S.C., Chan L.S. Influence of the design of square *p*<sup>+</sup> islands on the characteristics of 4H–SiC JBS. *IEEE Trans. Electron. Devices.* 2017. **64**. P. 1394–1398.
23. Huang L. Barrier inhomogeneities of platinum contacts to 4H–SiC. *Superlattices and Microstructures.* 2016. **100**. P. 648–655.
24. Latreche A. Conduction mechanisms of the reverse leakage current of 4H–SiC Schottky barrier diode. *Semicond. Sci. Technol.* 2018. <https://doi.org/10.1088/1361-6641/aaf8cb>.
25. Latreche A. and Ouennoughi Z. Modified Airy function method modeling of tunneling current for Schottky barrier diodes on silicon carbide. *Semicond. Sci. Technol.* 2013. **28**. P. 105003.
26. Zheng L., Joshi R.P. and Fazi C. Effects of barrier height fluctuations and electron tunnelling on the reverse characteristics of 6H–SiC Schottky contacts. *J. Appl. Phys.* 1999. **85**. P. 3701–3707.
27. Rhoderick E.H. and Williams R.H. *Metal–Semiconductor Contact*. Oxford: Oxford University Press, 1988.
28. Naik S.S., Reddy V.R. Temperature dependency and current transport mechanisms of Pd/*V*/*n*-type InP Schottky rectifiers. *Adv. Mat. Lett.* 2012. **3**. P. 188–196.
29. Turut A., Saglam M., Efeoglu H., Yalcin N., Yildirim M., Abay B. Interpreting the nonideal reverse bias CV characteristics and importance of the dependence of Schottky barrier height on applied voltage. *Physica B: Condensed Matter.* 1995. **205**. P. 41–50.
30. Vassilevski K.V., Nikitina I.P., Wright N.G. et al. Device processing and characterisation of high temperature silicon carbide Schottky diodes. *Microelectronic Engineering.* 2006. **83**. P. 150–154.
31. Ivanov P.A., Grekhov I.V., Potapov A.S. et al. Excess leakage currents in high-voltage 4H–SiC Schottky diodes. *Semiconductors.* 2010. **44**. P. 653–656.
32. Itoh A. and Matsunami H. Analysis of Schottky barrier heights of metal/SiC contacts and its possible application to high-voltage rectifying devices. *phys. status solidi (a)*. 1997. **162**. P. 389–408.
33. Roccaforte F. Richardson's constant in inhomogeneous silicon carbide Schottky contacts. *J. Appl. Phys.* 2003. **93**. P. 9137–9144.

#### Authors and CV



**Abdelhakim Latreche** is an assistant professor of the Department Material Sciences at Bordj Bou Arreridj University, Algeria. His main research interests include the electrical characterization and simulation of semiconductor devices, in particular, wide gap (SiC, Ga<sub>2</sub>O<sub>3</sub>,.....) Schottky barrier diodes.